J Intell Robot Syst (2018) 89:139–153
DOI 10.1007/s10846-017-0517-6

Collision Avoidance Based on Line-of-Sight Angle

Guaranteed Safety Using Limited Information About the Obstacle

Venanzio Cichella · Thiago Marinho · Dušan Stipanović · Naira Hovakimyan · Isaac Kaminer · Anna Trujillo

Received: 19 August 2016 / Accepted: 10 February 2017 / Published online: 16 March 2017

Abstract This paper focuses on the problem of collision avoidance for Unmanned Aerial Vehicles (UAVs). The dynamics of the UAV are modeled as a Dubins vehicle flying at constant altitude. The angular velocity is used as control input in order to avert a possible collision with a single obstacle, while the speed is left as an extra degree of freedom to achieve some temporal requirements. The proposed control algorithm uses only the line-of-sight angle as feedback: in this sense, the main contribution of this paper is providing a solution to the collision avoidance problem that can be used in situations where it is not possible to measure data such as position and velocity of the obstacle. A theoretical analysis of the result is provided, followed by simulation results that validate the efficacy of the control strategy.

Keywords Autonomy · Collision Avoidance · Line-of-sight angle

This work has been supported in part by AFOSR, NASA and NSF.

V. Cichella (✉) · T. Marinho · D. Stipanović · N. Hovakimyan
Coordinated Science Laboratory, University of Illinois at Urbana-Champaign, 1308 W Main St, Urbana, IL 61801, USA
e-mail: cichell2@illinois.edu

T. Marinho
e-mail: marinho@illinois.edu

D. Stipanović
e-mail: dusan@illinois.edu

N. Hovakimyan
e-mail: nhovakim@illinois.edu

I. Kaminer
Department of Mechanical and Aerospace Engineering, Naval Postgraduate School, Monterey, CA 93943, USA
e-mail: kaminer@nps.edu

A. Trujillo
Crew Systems and Aviation Operations Branch, NASA Langley Research Center, Hampton, VA 23666, USA
e-mail: a.c.trujillo@nasa.gov

1 Introduction

Unmanned Aerial Systems (UAS) have seen an exponential growth in development over the past two decades, with a wide range of potential applications, including aerial photography, communications and broadcast, critical infrastructure monitoring, and disaster response, to mention but a few. Due to the increased importance of UAS, much effort has been put into enabling piloted and Unmanned Aerial Vehicles (UAVs) to operate within the same airspace. One example is the NASA's UAS Integration in the National Airspace System (NAS) project,[1] which is developing technologies and concepts of use that

[1] https://www.nasa.gov/centers/armstrong/programs_projects/UAS_in_the_NAS/index.html

address one of the safety issues concerning the integration of UAVs into the NAS – detect and avoid (DAA) other crafts.

To address this challenge, a collision avoidance system, mounted on-board the UAV for time criticality, is necessary in order to avert a possible collision with obstacles. The collision avoidance system is comprised of three key enablers: (*i*) *sensing*, in charge of acquiring information and data of the obstacle; (*ii*) *detection*, which based on the information available about the obstacle, predicts whether a collision is going to take place or not; (*iii*) *avoidance*, which selects and enforces the proper evasive maneuver.

The potential success of a given collision avoidance system largely depends on the *sensing* capabilities, which are naturally characterized by technological limitations. Ground based systems (such as Traffic Alert and Collision Avoidance System (TCAS) [1], Automatic Dependent Surveillance-Broadcast (ADS-B) [2], and ground based radar systems [3, 4]) are recognized as the most accessible ways to provide the UAVs with information about other vehicles and obstacles flying in the airspace. However, the efficacy of these systems largely depends on the capability of the UAV to communicate in a reliable manner with a ground station. Hence, a faulty communication or a cyber attack may jeopardize the safety of the UAS. For this reason, in the last years there has been intense theoretical and experimental research on key enabling on-board technologies, which have led to commercial products that deliver high precision sensing capabilities [5–7]. Nevertheless, these sensing systems are usually expensive, large, heavy, and/or highly computational and power demanding. Simpler and low-cost solutions are also available; however, these provide less accurate data and reduced amount of reliable information (for example, the measured position and velocity of the obstacle might be unreliable, available only within relatively short ranges, or not available at all). The use of inexpensive sensing technologies is appealing to the low-cost UAS market, although it implies that more effort must be exerted to design *detection* and *avoidance* control strategies in order to ensure safety in presence of measurement errors and low amount of information.

The collision *detection* problem is still the topic of ongoing research in the fields of robotics, control engineering, and computer science (see [8–10] and references therein). Nevertheless, the problem of detecting a possible imminent collision is beyond the scope of this paper. In this work we focus on the development of a collision *avoidance* strategy that guarantees safety in the presence of limited amount of information about the obstacle. This avoidance strategy could then be coupled with a detection solution for minimally capable UAS, or could be presented to the operator and even automated.

Several approaches to collision avoidance have been proposed in the literature (see, for example, [11–25]). In [11], the authors show a method for designing avoidance controllers for a two-vehicle system with a solid and rigorous mathematical foundation. A certainty grid method was proposed in [12], while an occupancy grid method was presented in [26]. Virtual force field method was presented in [13] and artificial potential field was described in [27]. In [14, 28], the trajectory of the robot was modeled as an elastic material to avoid collision with objects. In [15], collision avoidance was introduced as a velocity cone concept, which has later been adopted in other publications as well (for example, see [16, 29, 30]). In [17, 19, 31], collision avoidance strategies based on a differential game theoretic approach are introduced, while a collision avoidance algorithm based on Lyapunov analysis is introduced in [20]. The latter exhibits guaranteed performance and safety even in the presence of sensing uncertainties. Finally, in [21–24, 32, 33] the authors address the vision-based collision avoidance problem, by assuming that the UAVs are equipped with passive sensors only. One of the features that the above solutions have in common is the basic assumption that the vehicles are capable of measuring the position (and velocity) of the obstacles. Even though some of these papers take into account sensing uncertainties, and assess the robustness of the proposed algorithm (e.g., [17]), they are not applicable to cases where the UAVs are equipped with sensors that are not capable of measuring the position at all.

The collision avoidance problem in the absence of position information of the obstacle has received considerably less attention in the literature. Few examples are [33–36]. In particular, in [33–35] it is shown that a collision can be avoided using image-based features (such as image area expansion, relative bearing rate), from which it is possible to estimate the range of UAV from obstacle [35], or the time to collision [33]. However, these solutions suffer from two main drawbacks. First, the image area expansion processing associated

with the motion of the obstacle needs to be carried out by apparatus (e.g. [37]) which are usually not available, by default, onboard of commercial low-cost platforms. Second, in these papers the collision avoidance algorithms are validated through experimental results only. The lack of a theoretical underpinning supporting the proposed solutions makes these works no weaker than other options, but less appealing to the control engineering and UAS marketing communities because of the potential certification difficulties. Finally, in [36] the authors propose a collision avoidance strategy that uses bearing-only measurements in order to avoid obstacles. However, the obstacles are assumed to be cylindrical static objects, and the theoretical approach does not address the problem of guaranteeing a minimum safety distance from the obstacle.

This paper proposes a solution to the collision avoidance problem that does not rely on position information of a moving obstacle, nor on its estimate. In particular, we show that *collision avoidance can be achieved upon knowledge of the line-of-sight (LOS) angle only*. The LOS angle can be obtained, for example, using a gimbaled camera, which can be built using low-cost commercial off-the-shelf components (e.g. a web camera and a pan-tilt gimbal capable of detecting an obstacle and lock it in the camera frame).

This work, initially presented in [38], is motivated by previous results from the same authors [39, 40], which addressed the problem of vision-based tracking and motion estimation of a ground target. We extend the work in [38] by considering a more general context in which an autonomous vehicle has to track a desired moving target, satisfy strict temporal constraints, and avoid pop-up obstacles. Trajectory tracking control laws are proposed for the speed and angular rate of the vehicle. A control law for the angular rate of the vehicle is proposed that enables the UAV to deviate from its desired position in order to avert a possible collision with obstacles. A proof based on Lyapunov analysis is presented, which provides a theoretical framework to assess the effectiveness of the proposed strategy, as well as intuitions on the correlation between the LOS angle, the distance between the UAV and the obstacle, and other parameters of interest (such as detection radius and velocity of the obstacle). Simulation results are also presented to validate the efficacy of the control law in challenging scenarios.

It is important to point out that the collision avoidance algorithm presented in this paper can be employed even in GPS denied environment, since the only data needed to avert a possible collision with a cooperative or uncooperative obstacle is the LOS angle relative to an inertial frame. We believe that further investigation in this direction will open the door to the integration of low-cost UAVs in the NAS, and will be a major enabler for the entire low-cost UAS sector.

The rest of the paper is organized as follows: we start stating the problem at hand in Section 2; a solution that solves the collision avoidance problem is proposed in Section 3, which also provides collision avoidance performance bounds and theoretical guarantees; Section 4 discusses simulation results; finally, the conclusions are summarized in Section 5.

2 Problem Formulation

In what follows we formulate the problem at hand in two-dimensional space. We restrict our approach to the 2D plane as a simplifying assumption; it should be noted that the proposed strategy can be easily integrated into existing collision avoidance systems, and be employed in cases where climb and descent maneuvers are not possible (e.g. due to close proximity to the ground, or to avoid busting altitude restrictions with climbs). A typical scenario addressed in this paper is depicted in Fig. 1, where a UAV is flying in the airspace when an unknown obstacle is detected. While the direction where the obstacle is coming from is known, the sensing system is not capable of measuring its position and velocity. In this case, it is preferred to perform an escaping maneuver to prevent a possible imminent collision, rather than waiting for the sensing system to gather accurate information about the obstacle, and having to perform a more hazardous maneuver later on.

We start by letting the position of the UAV at time t be defined as $p_{\mathrm{r}}(t) = [x_{\mathrm{r}}(t), y_{\mathrm{r}}(t)]^{\top}$. Then, let the motion of the vehicle be driven by

$$\mathcal{R}: \begin{cases} \dot{x}_{\mathrm{r}}(t) = V_{\mathrm{r}}(t)\cos\psi_{\mathrm{r}}(t), & x_{\mathrm{r},0} = x_{\mathrm{r}}(0) \\ \dot{y}_{\mathrm{r}}(t) = V_{\mathrm{r}}(t)\sin\psi_{\mathrm{r}}(t), & y_{\mathrm{r},0} = y_{\mathrm{r}}(0) \\ \dot{\psi}_{\mathrm{r}}(t) = \omega_{\mathrm{r}}(t) = \omega_{\mathrm{tr}}(t) + \omega_{\mathrm{ca}}(t), & \psi_{\mathrm{r},0} = \psi_{\mathrm{r}}(0) \end{cases} \tag{1}$$

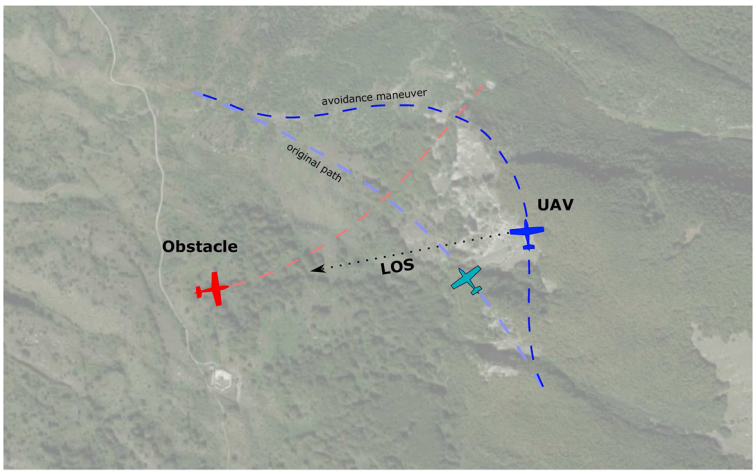

Fig. 1 A typical scenario in which a fixed-wing UAV has to perform an escaping maneuver to avoid collision with a pop-up obstacle

where $V_r(t)$ and $\psi_r(t)$ are the speed and heading angle of the vehicle, respectively, and $\omega_r(t) = \omega_{tr}(t)+\omega_{ca}(t)$ is its angular rate. Finally, let the motion of the obstacle, with position $p_o(t) = [x_o(t), y_o(t)]^\top$, be driven by

$$\mathcal{O} : \begin{cases} \dot{x}_o(t) = V_o(t)\cos\psi_o(t), & x_{o,0} = x_o(0) \\ \dot{y}_o(t) = V_o(t)\sin\psi_o(t), & y_{o,0} = y_o(0) \end{cases} \tag{2}$$

where $V_o(t)$, $\psi_o(t)$ are the obstacle's speed and heading angle. With this setup, the velocity of the vehicle $V_r(t)$ and the angular rate $\omega_{tr}(t)$ are used as extra degrees of freedom to achieve some mission specific requirements (such as trajectory tracking, way point navigation, temporal constraints), while the angular rate $\omega_{ca}(t)$ is used to avoid collision with the obstacle $\mathcal{O}$.

Next, in order to provide a rigorous formulation of the collision avoidance problem, we introduce a set of variables of interest. To this end, consider the UAV and obstacle relative 2D kinematics in an inertial frame $\mathcal{I}$ illustrated in Fig. 2 [39]. Let $\mathbf{V}_r(t) \in \mathbb{R}^2$ denote the UAV's velocity vector (with magnitude $V_r(t)$). Let $\mathbf{V}_o(t) \in \mathbb{R}^2$ be the velocity vector of the obstacle (with magnitude $V_o(t)$). Let $d(t) \in \mathbb{R}$ be the distance between the UAV and the obstacle. Let $\lambda(t) \in \mathbb{R}$ be the LOS angle, let $\boldsymbol{\lambda}(t) \in \mathbb{R}^2$ denote the LOS vector, and let $\boldsymbol{\lambda}_p(t) \in \mathbb{R}^2$ be the vector perpendicular to $\boldsymbol{\lambda}(t)$. Finally, let $\eta(t) \in \mathbb{R}$ denote the angle between $\boldsymbol{\lambda}_p(t)$ and $\mathbf{V}_r(t)$, which can be written as

$$\eta(t) = \psi_r(t) - \left(\lambda(t) - \frac{\pi}{2}\right). \tag{3}$$

The variable $\eta(t)$ plays a crucial role, as it captures the key idea pursued in this paper. In fact, the collision avoidance objective presented in this work is based on driving this variable to a neighborhood of zero. By doing so, we force the UAV to travel along a

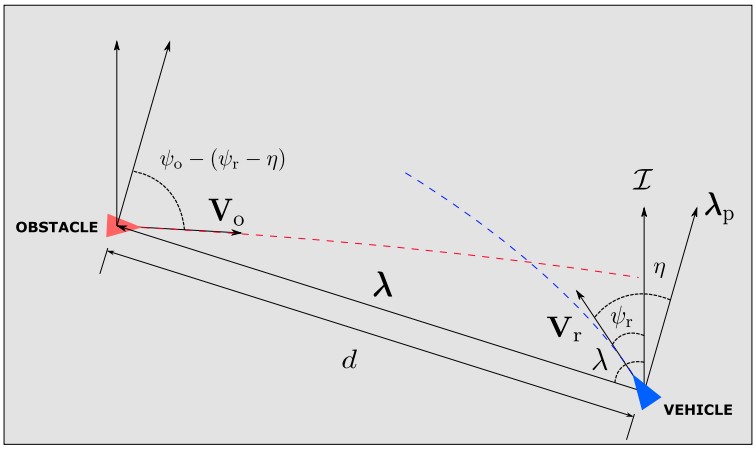

Fig. 2 Geometry of the collision avoidance problem

direction perpendicular to the position of the obstacle with respect to the UAV. In other words, if $\eta(t) = 0$, it follows from (3) that the angle between the UAV's velocity vector and the LOS vector equals $\frac{\pi}{2}$ rad. Of course, this constitutes only part of the collision avoidance objective. In fact, to successfully achieve avoidance, the control law must ensure that the UAV maintains a certain safety distance away from the obstacle. Clearly, this can be achieved by guaranteeing that the distance between the obstacle and the UAV, $d(t)$, satisfies $d(t) \geq d_{\text{sf}}$, where $d_{\text{sf}} > 0$ is a given constant parameter which depends on the dimension of the vehicle, dimension of the obstacle, and other safety requirements.

At last, before providing a formal statement of the problem at hand, we formulate a set of assumptions that the vehicle and obstacle must satisfy. In particular, we assume that the speed and angular velocity of the vehicle do not violate the prescribed bounds $V_{\text{r,min}}, V_{\text{r,max}}, b_{\text{tr}} > 0$, i.e.

$$V_{\text{r,min}} \leq V_{\text{r}}(t) \leq V_{\text{r,max}}, \tag{4}$$

$$|\omega_{\text{tr}}| \leq b_{\text{tr}}. \tag{5}$$

Similarly, we assume that the velocity of the obstacle is bounded as follows:

$$V_{\text{o,min}} \leq V_{\text{o}}(t) \leq V_{\text{o,max}}, \tag{6}$$

where $V_{\text{o,min}} \geq 0$ and $V_{\text{o,max}} > 0$. Then, the collision avoidance control problem can be defined as follows:

Problem 1 *Consider a UAV and an obstacle. Let their dynamics, given by* Eqs. 1 *and* 2*, satisfy the bounds given by* Eqs. 4, 5 *and* 6*. Then, the collision avoidance objective is to derive a control law for* $\omega_{ca}(t)$ *such that the distance between the UAV and the obstacle is always greater than a given safety distance, i.e.* $d(t) \geq d_{sf}$.

3 Main Result

This section is concerned with the solution to Problem 1. Nevertheless, the main challenge is to formulate a control algorithm for the angular rate $\omega_{\text{ca}}(t)$ that relies only on the knowledge of the UAV's heading angle $\psi_{\text{r}}(t)$, obtained from onboard localization systems such as an inertial measurement unit typical for modern autopilots, and the LOS angle $\lambda(t)$, which can be obtained by an image processing software (centroid position in the camera frame). In this sense, the crucial part of the proposed approach is to formulate a control law that ensures that the distance $d(t)$ between the UAV and the obstacle remains bounded away from d_{sf}, even without knowing the actual distance $d(t)$. To this end, we proceed by stating the main result of this paper, which can be summarized in the following control law for the angular rate of the vehicle:

$$\omega_{\text{ca}}(t) = -k\eta(t), \tag{7}$$

where $k > 0$ is a control gain to be selected. The intuition behind the above control law is as follows: by applying the angular rate given by Eq. 7, the UAV is forced to travel in a direction tangential to a circle centered at the obstacle's position. This, in turn, suggests that under some conditions on the obstacle's and the vehicle's dynamics, the UAV will successfully avert collision. The remaining of this section is aimed at providing a theoretical basis that supports this intuition. In particular, the objective is to demonstrate that the control law in Eq. 7 guarantees safety, and that a minimum safety distance between the UAV and the obstacle can be ensured. This fundamental result is stated in the following Lemma:

Lemma 1 *Consider an autonomous vehicle moving with speed* $V_r(t)$ *satisfying the bound given by* Eq. 4*, and a moving obstacle with speed satisfying the bound in* Eq. 6*. Assume that at time* $t = t_0$ *an obstacle is detected at (unknown) distance* $d(t_0) = R$*, where* R *is denoted as detection radius. Let the commanded angular rate of the UAV at time* $t \in [t_0, t_f]$ *be*

$$\omega_r(t) = \omega_{tr}(t) + \omega_{ca}(t),$$

where $\omega_{tr}(t)$ *satisfies the bound given by* Eq. 5*, and* $\omega_{ca}(t)$ *is given by* Eq. 7*. Let the collision avoidance state* $x(t) = [\eta(t)/d_d, 1/d(t)]^\top$ *at time* $t = t_0$ *satisfy*

$$x(t_0) = [\eta(t_0)/d_d, 1/R]^\top \in \Omega_v, \tag{8}$$

with

$$\Omega_v \triangleq \{x(t) : ||x(t)|| \leq c_d/d_d\}, \tag{9}$$

for some $c_d, d_d > 0$ *satisfying* Eq. 16 *and*

$$\frac{c_d}{d_d} \leq \frac{1}{d_{sf}}, \tag{10}$$

for any $d_{sf} > 0$. Let the control gain verify

$$k > max\left(\frac{2V_r/d_d}{\sqrt{4V_r/V_{r,min}-1}}, 1\right).$$

Finally, assume that the bounds in Eqs. 5 *and* 6 *satisfy*

$$\frac{V_{o,max}c_d\sqrt{1+c_d^2}}{\lambda_v d_d} + \frac{b_{tr}}{2\lambda_v} < c_d \tag{11}$$

for some $\lambda_v > 0$. Then, the following result holds:

$$d(t) \geq d_{sf}, \quad \forall t \in [t_0, t_f].$$

Proof The proof of Lemma 1 is given in Appendix A. □

Remark 1 The variables c_d and d_d define the domain of attraction Ω_v (see Eq. 8) within which the collision avoidance state remains for all times. These variables satisfy the bound given by Eq. 16 for a suitable choice of the control gain k. Then, if the velocity of the obstacle, the heading angle rate, and the initial state satisfy Eqs. 8 and 11, the collision avoidance state never leaves Ω_v. In turn, if c_d and d_d verify Eq. 10, this implies that the vehicle remains within the safety distance d_{sf}. Notice that conditions (8) and (11) give an algebraic relationship between the detection radius and the velocity of the obstacle. For example, for fixed c_d, a large detection radius would relax the assumption given in Eq. 8 by allowing larger values for d_d. In turn, this implies that the obstacle can travel faster (see Eq. 11). Following a similar argument, if the obstacle is detected only in the proximity of the UAV, Eq. 11 suggests that avoidance is ensured only if the velocity of the obstacle is small enough. In this sense, the theoretical results are in agreement with the intuition that fast obstacles can be avoided only if detected far ahead.

Remark 2 It is straightforward to verify that a control gain k and control parameters c_d, d_d that satisfy conditions (10) and (16) can always be found. However, such values can result in bounds for the speed of the obstacle, detection radius, and angular rate of the vehicle that are conservative (see Eqs. 8 and 11), thus limiting the range of potential collisions that can be (theoretically) avoided. This is not surprising for the following reasons: (i) the approach tackles the problem at the kinematic level. By considering more specific dynamic models for the vehicle and the obstacle (e.g. multirotors, which is the objective of future research), the theoretical analysis would provide less conservative bounds; (ii) we choose to adjust exclusively the angular rate of the vehicle to avert collisions with obstacles, while leaving the linear speed as an extra degree of freedom to satisfy temporal mission requirements. Doing so, the proposed approach extends previous results from the same authors, in which the speed of multiple cooperative UAVs is adjusted in order to achieve coordination and ensure inter-vehicle safety [41, 42]; (iii) the theoretical proof is based on a Lyapunov approach, which on one hand offers rigorous stability results, but on the other hand provides bounds that are far more conservative than the realistic ones. This is discussed in the simulation results section, which shows the effectiveness of the proposed strategy even in scenarios where the performance bounds are violated.

4 Simulation Results

This section presents two different simulation scenarios. In both cases, the UAV and the obstacle are assumed to be small fixed-wing UAVs with speed limits

$$\begin{aligned} 18\ \text{m/s} = V_{\mathrm{r,min}} \leq V_{\mathrm{r}} \leq V_{\mathrm{r,max}} = 32\ \text{m/s}, \\ 18\ \text{m/s} \leq V_{\mathrm{o}} \leq 32\ \text{m/s}. \end{aligned} \tag{12}$$

Saturation bounds on the angular rates of the vehicles are also imposed:

$$-0.2\ \text{rad/s} \leq \omega_{\mathrm{r}} \leq 0.2\ \text{m/s}, \quad -0.2\ \text{m/s} \leq \omega_{\mathrm{o}} \leq 0.2\ \text{m/s}, \tag{13}$$

while the collision avoidance control gain is selected as $k = 1.1$.

4.1 First Scenario

A fixed-wing UAV is wandering in the airspace on a straight line with speed $V_{\mathrm{r}} = 23$ m/s. At time $t_1 = 33$ s an obstacle is detected from a direction given by $\lambda(t_1) = 2.05$ rad, with unknown position and velocity. The vehicle is required to perform a safety maneuver to avoid a possible collision (or to reduce the risk of collision until additional information about the obstacle is available). Given the UAV speed limits, and for a

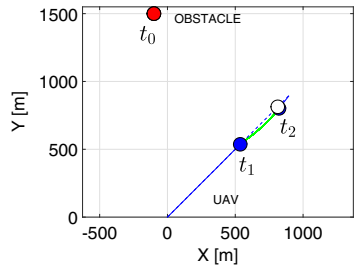

(a) Static obstacle.

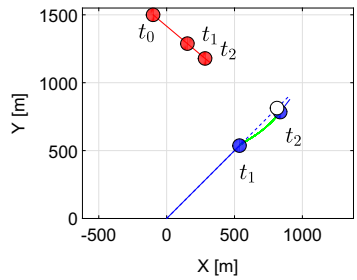

(b) Speed of the obstacle $V_o = 10$m/s.

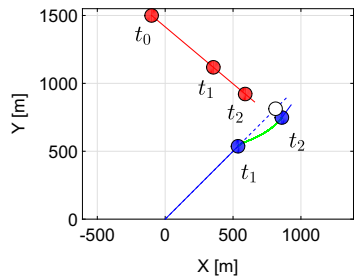

(c) Speed of the obstacle $V_o = 18$m/s.

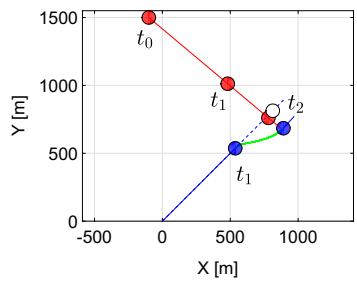

(d) Speed of the obstacle $V_o = 23$m/s.

Fig. 3 UAV (*blue line*) and obstacle (*red line*) two-dimensional paths. The *circles* indicate the position of the UAV (*blue*) and obstacle (*red*) at times $t_0 = 0s$, $t_1 = 33$ s, and $t_2 = 50$ s. The *white circle* indicates the position of the UAV at time t_2 if the collision avoidance maneuver were not performed

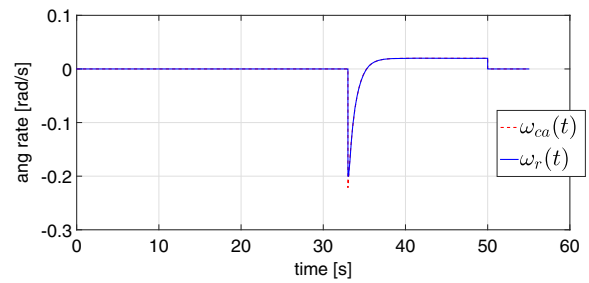

(a) Static obstacle.

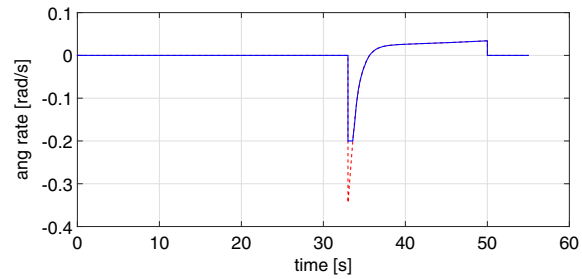

(b) Speed of the obstacle $V_o = 10$m/s.

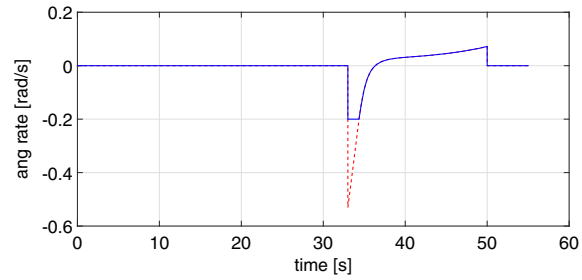

(c) Speed of the obstacle $V_o = 18$m/s.

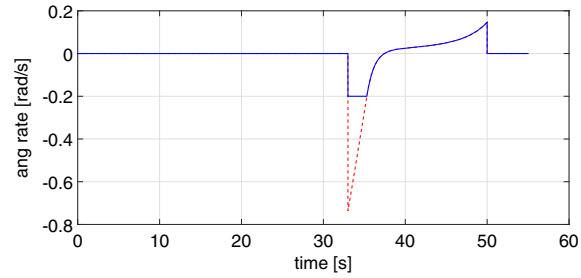

(d) Speed of the obstacle $V_o = 23$m/s.

Fig. 4 Angular rate of the vehicle (*blue line*) and collision avoidance control input $\omega_{ca}(t)$ (*red line*)

required safety distance $d_{sf} = 50$ m, parameters $c_d = 0.3033$ and $d_d = 40$ can be chosen that satisfy Eqs. 10 and 16, where $\lambda_v = \frac{\lambda_{min}(W)}{20\lambda_{max}(P)} = 0.0116$ in Eq. 16 is selected. According to Lemma 1, such parameters suggest that only slow moving obstacles can be avoided (with speed as low as $V_o = 0.4430$ m/s). This is the case of Fig. 3a, where the obstacle is assumed to

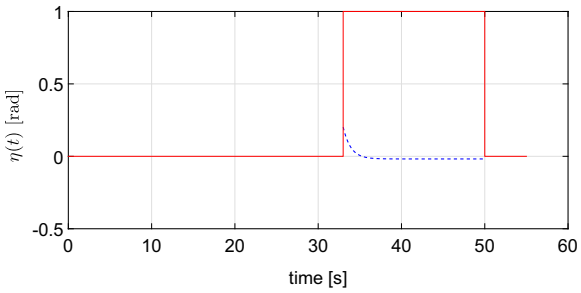

(a) Static obstacle.

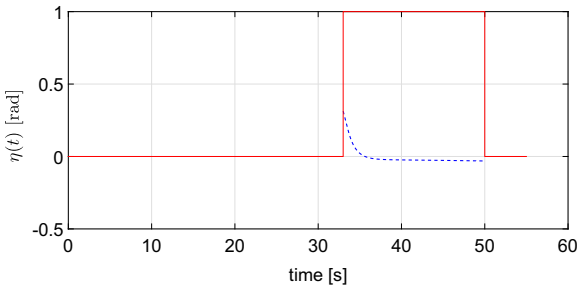

(b) Speed of the obstacle $V_o = 10\text{m/s}$.

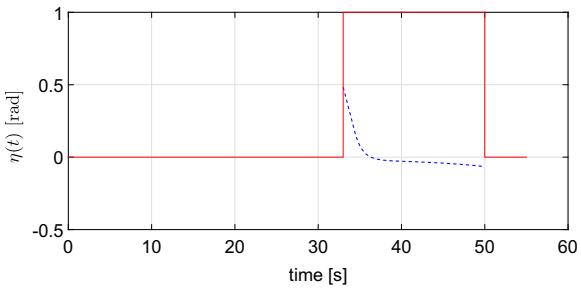

(c) Speed of the obstacle $V_o = 18\text{m/s}$.

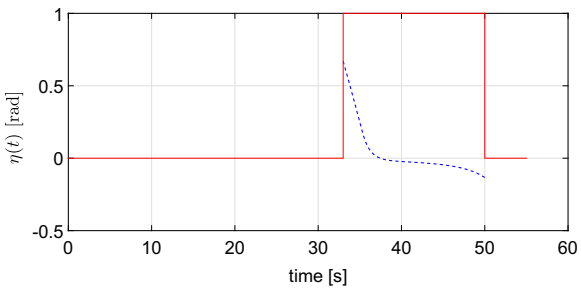

(d) Speed of the obstacle $V_o = 23\text{m/s}$.

Fig. 5 Collision avoidance error $\eta(t)$ (*dashed blue line*) and collision avoidance switch (*red line*)

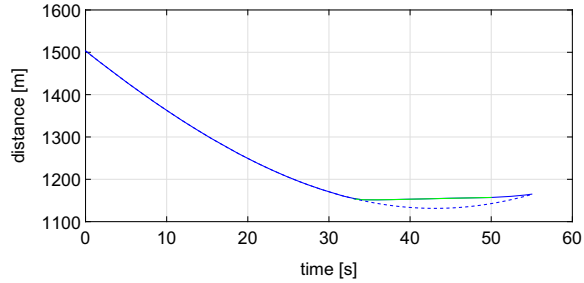

(a) Static obstacle.

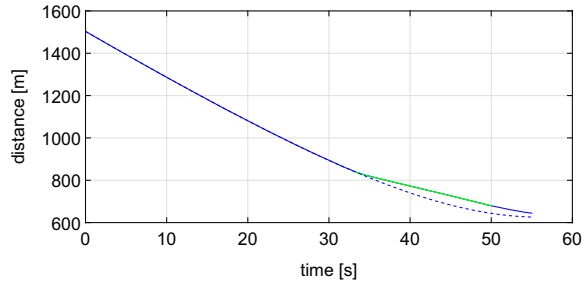

(b) Speed of the obstacle $V_o = 10\text{m/s}$.

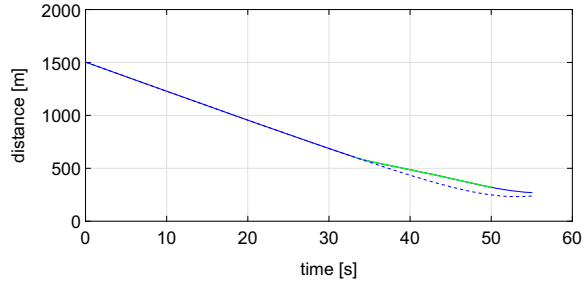

(c) Speed of the obstacle $V_o = 18\text{m/s}$.

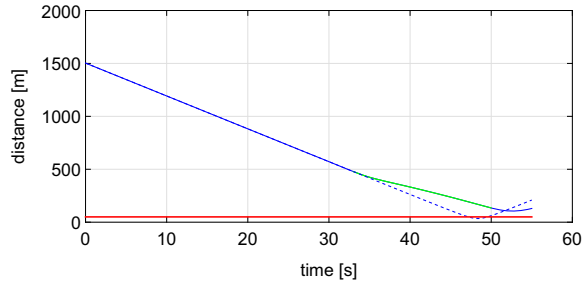

(d) Speed of the obstacle $V_o = 23\text{m/s}$.

Fig. 6 Actual distance between the UAV and the obstacle (*solid line*). The *dashed line* shows the same distance in the case where the collision avoidance control law is turned off. The green segments indicate the time ranges when the collision avoidance maneuvers take place. The *red line* shows the minimum safety distance requirement

be static and thus its speed satisfies Eq. 11, and where the initial states $\eta(t_1) = 0.2$ rad and $d(t_1) = 1155$ m satisfy Eq. 8. Nevertheless, Fig. 3a–d show that the proposed solution is effective even when such bounds are violated, as pointed out in Remark 2. In particular, Fig. 3b, c, and d illustrate three scenarios in which

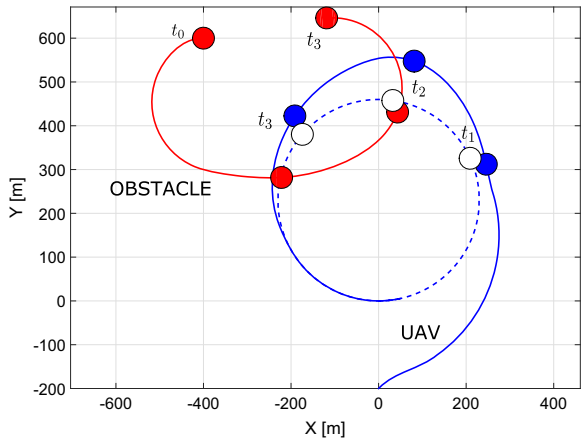

Fig. 7 UAV (*solid blue line*), virtual target (*dashed blue line*) and obstacle (*red line*) two-dimensional paths. The circles indicate the position of the UAV (*blue*), virtual target (*white*) and obstacle (*red*) at times $t_0 = 0s$, $t_1 = 20s$, and $t_3 = 30$ s

the obstacle travels on a straight line at speeds $V_o = 10, 18, 23$ m/s, respectively. It can be noted that the UAV performs more aggressive maneuvers for higher speeds of the obstacle, and ultimately avoids collision. The control effort for the four cases described above is depicted in Fig. 4, and it is compared with the actual angular rate of the vehicle subject to the saturation bound given by Eq. 13. The time history of the collision avoidance state $\eta(t)$ is illustrated in Fig. 5, which also highlights the time ranges when the collision avoidance control law is activated. As expected, $\eta(t)$ converges to a neighborhood of zero when the collision avoidance algorithm is turned on. Finally, Fig. 6 depicts the distance between the UAV and the obstacle, which remains above the safety limit $d_{sf} = 50$ m.

4.2 Second Scenario

In this scenario, a fixed-wing UAV is tasked to inspect an area by following a circular path. The desired trajectory (or *virtual target*) to be followed is given by

$$\begin{cases} \dot{x}_{vt}(t) = V_{vt}(t)\cos\psi_{vt}(t) \\ \dot{y}_{vt}(t) = V_{vt}(t)\sin\psi_{vt}(t), \\ \dot{\psi}_{vt}(t) = \omega_{vt}(t), \end{cases}$$

with $x_{vt}(0) = 0$, $y_{vt}(0) = 0$, $\psi_{vt}(0) = 0$, $V_{vt}(t) = 23$ m/s, and $\omega_{vt}(t) = 0.1$ rad/s, $\forall t \geq 0$. Thus, trajectory tracking control laws need to be formulated for the speed of the UAV $V_r(t)$ and the angular rate $\omega_{tr}(t)$ that enable the vehicle to follow the above virtual target while satisfying the bounds in Eqs. 4 and 5.

To this end, motivated by [43], we let the speed of the vehicle be governed by

$$V_r = \text{sat}\left(V_{vt}\cos(\psi_{vt}-\psi_r) + \eta_v(\cos(\psi_r)(x_{vt}-x_r) + \sin(\psi_r)(y_{vt}-y_r)\right), V_{r,\min}, V_{r,\max}\Big), \quad (14)$$

and the angular rate be

$$\omega_{tr} = \text{sat}\left(\omega_{vt} + \eta_\omega\left(m(\psi_{vt}-\psi_r) + \frac{\cos(\psi_r)(y_{vt}-y_r) - \sin(\psi_r)(x_{vt}-x_r)}{\sqrt{(x_{vt}-x_r)^2 + (y_{vt}-y_r)^2 + 1}}\right), -b_{tr}, b_{tr}\right), \quad (15)$$

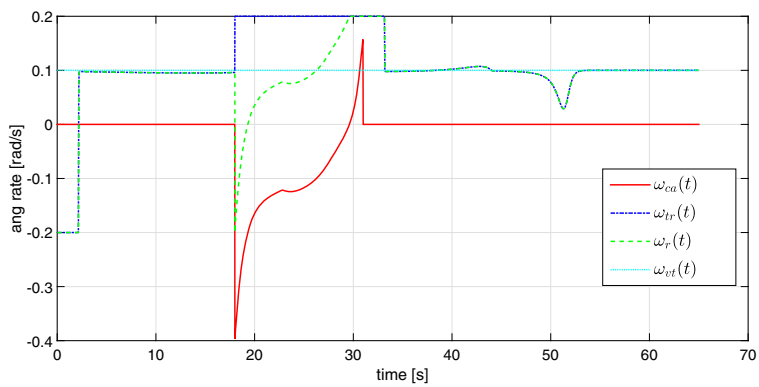

Fig. 8 Angular rate of the UAV

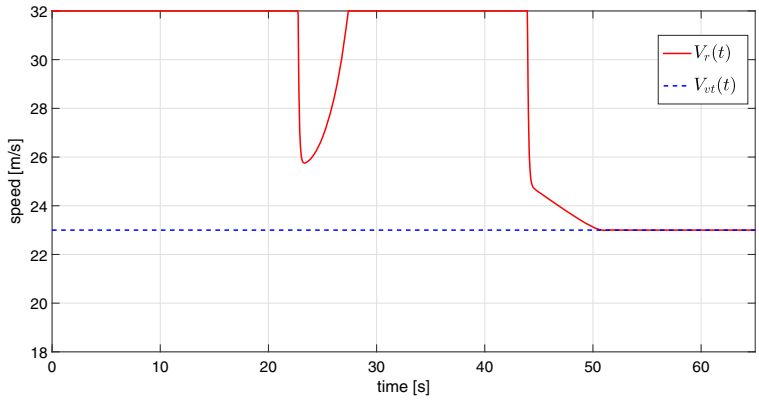

Fig. 9 UAV and virtual target's speed

for some trajectory tracking control gains $\eta_{\mathrm{v}}, \eta_{\omega}$, $m > 0$, and with the saturation function defined as

$$\mathrm{sat}(a, b, c) = \begin{cases} b & a < b \\ a & b \le a \le c \\ c & a > c. \end{cases}$$

In this simulation the trajectory tracking control gains are selected as follows:

$$\eta_{\mathrm{v}} = 10, \quad \eta_{\omega} = 10, \quad m = 7,$$

while the angular rate saturation limit is set to $b_{\mathrm{tr}} = 0.2$. The UAV is initially positioned at $x_{\mathrm{r}}(0) = 0$, $y_{\mathrm{r}}(0) = -200$ and approaches the desired trajectory by virtue of the above control laws (see Fig. 7).

In order to test our solution in a more challenging scenario, an obstacle is simulated as an attacker, which chases the UAV by virtue of the following control algorithms for the speed and angular rate:

$$\begin{aligned} V_{\mathrm{o}} &= \mathrm{sat}\left(\eta_{\mathrm{vo}}(\cos(\psi_{\mathrm{o}})(x_{\mathrm{r}} - x_{\mathrm{o}}) \right. \\ &\quad \left. + \sin(\psi_{\mathrm{o}})(y_{\mathrm{r}} - y_{\mathrm{o}})), V_{\mathrm{r,min}}, V_{\mathrm{r,max}}\right), \\ \omega_{\mathrm{o}} &= \mathrm{sat}\left(\eta_{\omega\mathrm{o}}\left(\frac{\cos(\psi_{\mathrm{o}})(y_{\mathrm{r}} - y_{\mathrm{o}}) - \sin(\psi_{\mathrm{o}})(x_{\mathrm{r}} - x_{\mathrm{o}})}{\sqrt{(x_{\mathrm{r}} - x_{\mathrm{o}})^2 + (y_{\mathrm{r}} - y_{\mathrm{o}})^2} + 1}\right)\right. \\ &\quad \left. - b_{\mathrm{tr}}, b_{\mathrm{tr}}\right), \end{aligned}$$

with $\eta_{\mathrm{vo}} = \eta_{\omega\mathrm{o}} = 10$. Note that the differences between the above control laws and the tracking control laws given by Eqs. 14 and 15 are due to the fact that the obstacle is assumed to know the UAV's position, but not its heading angle and angular speed.

At time $t_1 = 18$ s the UAV detects the obstacle and starts an escaping maneuver by activating the proposed collision avoidance control law. Figure 7 illustrates the two-dimensional paths of the UAV, virtual

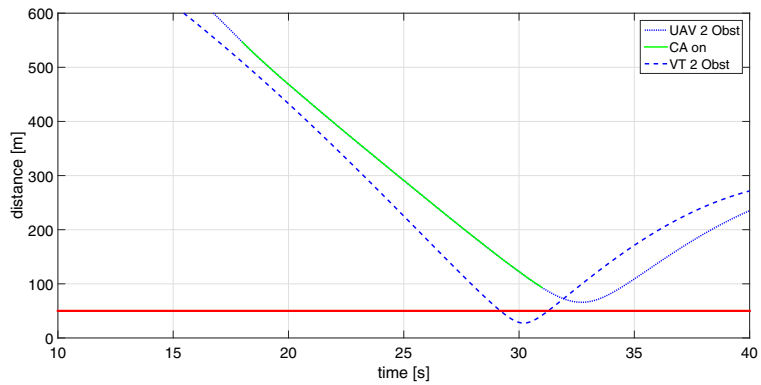

Fig. 10 Distance between UAV and obstacle (*solid line*) and between virtual target and obstacle (*dashed line*). The *green* segment indicates the time range when the collision avoidance maneuver takes place

target, and obstacle while the collision avoidance maneuver takes place. The control effort is shown in Fig. 8, which compares the angular rates of the vehicle and the virtual target. While performing the escaping maneuver to avoid the obstacle, the vehicle also speeds up in order to catch up with the virtual target (see Fig. 9). Finally, Fig. 10 illustrates the distance between the UAV and the obstacle, thus validating the efficacy of the collision avoidance strategy in the proposed scenario.

5 Conclusion

This paper proposed a collision avoidance strategy for UAVs. The angular rate of the vehicle is used as control input to avert a possible collision with a single pop-up obstacle. The main contribution of this work is to provide an avoidance algorithm which uses only the line-of-sight angle as feedback and the angular rate as control input. A Lyapunov-based analysis provides conditions on the velocity of the obstacle and detection radius, under which safety is theoretically guaranteed. Simulation results are presented to validate the proposed strategy.

Appendix A

Proof of Lemma 1

In what follows, we use tools from nonlinear analysis to prove that the distance between the vehicle and the obstacle remains lower bounded for all times. The proof is motivated by [39], where the authors dealt with the vision based tracking control problem. Before stating with the proof, let us introduce the positive constants $c_d, d_d > 0$. Let c_d and d_d satisfy the following condition:

$$\frac{c_d^2}{d_d} < \frac{\lambda_{\min}(W) - 2\lambda_v \lambda_{\max}(P)}{2\sqrt{2}\lambda_{\max}(P) V_{r,\max}}, \tag{16}$$

with

$$P = \begin{bmatrix} \frac{d_d}{V_{r,\min}} k & 1 \\ 1 & \frac{d_d}{V_{r,\min}} k \end{bmatrix}, \tag{17}$$

$$W = \begin{bmatrix} 2k^2 \frac{d_d}{V_{r,\min}} - 2\frac{V_r}{d_d} & k \\ k & 2\frac{V_r}{d_d} \end{bmatrix}, 0 < \lambda_v < \frac{\lambda_{\min}(W)}{2\lambda_{\max}(P)}.$$

Now, we express the rotational speed of the LOS as

$$\dot{\lambda}(t) = \frac{V_{\mathrm{r}}(t)\cos(\eta(t))}{d(t)} - \frac{V_{\mathrm{o}}(t)\cos(\psi_{\mathrm{o}}(t) - (\psi_{\mathrm{r}}(t) - \eta(t)))}{d(t)}, \tag{18}$$

which is obtained by projecting the UAV and obstacle velocity vectors onto the vector perpendicular to the LOS (see Fig. 2). Therefore, using the above equation, one can compute the derivative of (3) as

$$\dot{\eta}(t) = -\frac{V_{\mathrm{r}}(t)\cos(\eta(t)) - V_{\mathrm{o}}(t)\cos(\psi_{\mathrm{o}}(t) - (\psi_{\mathrm{r}}(t) - \eta(t)))}{d(t)} + \omega_{\mathrm{r}}(t).$$

Then, by projecting the UAV's velocity vector onto the LOS, we can express the derivative of $d(t)$ as follows:

$$\dot{d}(t) = -V_{\mathrm{r}}(t)\sin(\eta(t)) + V_{\mathrm{o}}(t)\sin(\psi_{\mathrm{o}}(t) - (\psi_{\mathrm{r}}(t) - \eta(t))).$$

By defining $x_1(t) = \eta(t)/d_d$ and $x_2(t) = 1/d(t)$, we can write the following system of dynamic equations:

$$\begin{cases} \dot{x}_1(t) = -\frac{V_{\mathrm{r}}(t)\cos(x_1(t)d_d)}{d_d}\, x_2(t) + \frac{\omega_{\mathrm{r}}(t)}{d_d} + \frac{V_{\mathrm{o}}(t)\cos(x_1(t)d_d - \psi_{\mathrm{r}}(t) + \psi_{\mathrm{o}}(t))}{d_d} x_2(t) \\ \dot{x}_2(t) = x_2^2(t)\ V_{\mathrm{r}}(t)\sin(x_1(t)d_d) - x_2^2(t) V_{\mathrm{o}}(t)\sin(x_1(t)d_d - \psi_{\mathrm{r}}(t) + \psi_{\mathrm{o}}(t)). \end{cases} \tag{19}$$

Substituting $\omega_{\mathrm{r}}(t) = \omega_{\mathrm{tr}}(t) + \omega_{\mathrm{ca}}(t)$, with $\omega_{\mathrm{ca}}(t)$ defined in Eq. 7, we obtain

$$\begin{cases} \dot{x}_1 = -\frac{V_{\mathrm{r}}\cos(x_1 d_d)}{d_d}\, x_2 - k x_1 + \frac{\omega_{\mathrm{tr}}}{d_d} + \frac{V_{\mathrm{o}}\cos(x_1 d_d - \psi_{\mathrm{r}} + \psi_{\mathrm{o}})}{d_d} x_2 \\ \dot{x}_2 = x_2^2\ V_{\mathrm{r}}\sin(\eta) - x_2^2 V_{\mathrm{o}}\sin(x_1 d_d - \psi_{\mathrm{r}} + \psi_{\mathrm{o}}), \end{cases}$$

where the dependence on time is neglected for the sake of simplicity. After simple algebraic manipulations we can rewrite the previous system of equations as

$$\dot{x} = A_x x + f(x) + \begin{bmatrix} \frac{\omega_{\mathrm{tr}}}{d_d} \\ 0 \end{bmatrix},$$

where $x = [x_1, x_2]^\top$,

$$A_x = \begin{bmatrix} -k & -V_{\mathrm{r}}/d_d \\ V_{\mathrm{r}}/d_d & 0 \end{bmatrix},$$

$$f(x) = \begin{bmatrix} V_{\mathrm{r}} x_2 (1 - \cos(x_1 d_d))/d_d \\ V_{\mathrm{r}} x_2^2 \sin(x_1 d_d) - \frac{V_{\mathrm{r}}}{d_d} x_1 \end{bmatrix} + \begin{bmatrix} V_{\mathrm{o}} x_2 \cos(x_1 d_d - \psi_{\mathrm{r}} + \psi_{\mathrm{o}})/d_d \\ -V_{\mathrm{o}} x_2^2 \sin(x_1 d_d - \psi_{\mathrm{r}} + \psi_{\mathrm{o}}) \end{bmatrix}.$$

Next, one can show that $\forall x \in \Omega_v$, $f(x)$ satisfies the following bound

$$||f(x)|| \leq \sqrt{2} \frac{V_{\mathrm{r}}}{d_d} c_d^2 ||x|| + \frac{V_{\mathrm{o,max}} c_d}{d_d^2} \sqrt{(1 + c_d^2)}. \quad (20)$$

For a proof of inequality (20) see Appendix B. Now consider the following Lyapunov function [44]

$$V(x) = x^\top P x, \quad P = \begin{bmatrix} \frac{d_d}{V_{\mathrm{r,min}}} k & 1 \\ 1 & \frac{d_d}{V_{\mathrm{r,min}}} k \end{bmatrix}. \quad (21)$$

Letting

$$W = \begin{bmatrix} 2k^2 \frac{d_d}{V_{\mathrm{r,min}}} - 2\frac{V_{\mathrm{r}}}{d_d} & k \\ k & 2\frac{V_{\mathrm{r}}}{d_d} \end{bmatrix} > 0,$$

and noting that $A_x^\top P + P A_x = -W$, the derivative of the Lyapunov function can be computed as

$$\dot{V} = -x^\top W x + 2 f^\top(x) P x + 2 \begin{bmatrix} \frac{\omega_{\mathrm{tr}}}{d_d} \\ 0 \end{bmatrix}^\top P x.$$

Defining λ_v such that $0 < \lambda_v < \frac{\lambda_{\min}(W)}{2\lambda_{\max}(P)}$, and recalling the bounds in Eqs. 16 and 20, one can write

$$\begin{aligned} \dot{V} &\leq -\lambda_{\min}(W)||x||^2 + 2\lambda_{\max}(P)||f||||x|| + 2\frac{b_{\mathrm{tr}}}{d_d}\lambda_{\max}(P)||x|| \\ &\leq -\left(\lambda_{\min}(W) - 2\sqrt{2}\lambda_{\max}(P)\frac{V_{\mathrm{r}}}{d_d}c_d^2\right)||x||^2 \\ &\quad + 2\frac{\lambda_{\max}(P)}{d_d}\left(\frac{V_{\mathrm{o,max}} c_d}{d_d}\sqrt{(1+c_d^2)} + b_{\mathrm{tr}}\right)||x|| \\ &\leq -2\lambda_v \lambda_{\max}(P)||x||^2 \\ &\quad + 2\left(\frac{V_{\mathrm{o,max}} c_d}{d_d^2}\sqrt{(1+c_d^2)} + \frac{b_{\mathrm{tr}}}{d_d}\right)\lambda_{\max}(P)||x|| \\ &\leq -2\lambda_{\max}(P)||x||\left(\lambda_v||x|| - \frac{V_{\mathrm{o,max}} c_d}{d_d^2}\sqrt{(1+c_d^2)} - \frac{b_{\mathrm{tr}}}{d_d}\right). \end{aligned} \quad (22)$$

It follows that $\dot{V} < 0$ if

$$\frac{V_{\mathrm{o,max}} c_d}{\lambda_v d_d^2}\sqrt{(1+c_d^2)} + \frac{b_{\mathrm{tr}}}{\lambda_v d_d} < ||x||. \quad (23)$$

Finally, we can conclude that if $V_{\mathrm{o,max}}$ and b_{tr} are sufficiently small and satisfy condition (11), then $||x|| \leq \frac{c_d}{d_d}$, $\forall t \geq 0$, which implies

$$|x_2| = \left|\frac{1}{d}\right| \leq \frac{c_d}{d_d}.$$

The previous inequality can be rewritten as

$$d \geq \frac{d_d}{c_d}.$$

Thus, since c_d and d_d satisfy condition (10), i.e. $d_d \geq c_d d_{\mathrm{sf}}$, the following result holds

$$d(t) \geq d_{\mathrm{sf}}, \quad \forall t \geq 0,$$

which completes the proof.

Appendix B

Proof of Inequality (20)

First, let $f(x) = f_r(x) + f_o(x)$, where

$$f_r(x) = \begin{bmatrix} V_{\mathrm{r}} x_2 (1 - \cos(x_1 d_d))/d_d \\ V_{\mathrm{r}} x_2^2 \sin(x_1 d_d) - \frac{V_{\mathrm{r}}}{d_d} x_1 \end{bmatrix},$$

and

$$f_o(x) = \begin{bmatrix} V_{\mathrm{o}} x_2 \cos(x_1 d_d - \psi_{\mathrm{r}} + \psi_{\mathrm{o}})/d_d \\ -V_{\mathrm{o}} x_2^2 \sin(x_1 d_d - \psi_{\mathrm{r}} + \psi_{\mathrm{o}}) \end{bmatrix}.$$

To prove that the first term is bounded by

$$||f_r(x)|| \leq \sqrt{2}\frac{V_{\mathrm{r}}}{d_d} c_d^2 ||x||, \quad (24)$$

we start noticing that, since

$$\lambda_{\min}(P)||x||^2 \leq x^\top P x \leq \lambda_{\max}(P)||x||^2,$$

we have that $x \in \Omega_v$ implies $||x|| \leq \frac{c_d}{d_d}$. Applying the identity $1 - \cos(\eta) = 2\sin^2\left(\frac{\eta}{2}\right)$ to $f_r(x)$ we obtain

$$\begin{aligned} f_r(x) &= \begin{bmatrix} V_{\mathrm{r}} x_2 (1 - \cos(x_1 d_d))/d_d \\ V_{\mathrm{r}} x_2^2 \sin(x_2 d_d) - \frac{V_{\mathrm{r}}}{d_d} x_1(t) \end{bmatrix} \\ &= \frac{V_{\mathrm{r}}}{d_d^2}\begin{bmatrix} 2 d_d x_2 \sin^2\left(\frac{\eta}{2}\right) \\ d_d^2 x_2^2 \sin(\eta) - \eta \end{bmatrix}. \end{aligned}$$

Then,

$$
\begin{aligned}
||f_r(x)||^2 &= \frac{V_r^2}{d_d^4}\left(4d_d^2x_2^2\sin^4\left(\frac{\eta}{2}\right)+(d_d^2x_2^2\sin\eta-\eta)^2\right)\\
&\le \frac{V_r^2}{d_d^4}\left(\frac{c_d^2\eta^4}{4}+(c_d^2\sin\eta-\eta)^2\right)\\
&= \frac{V_r^2}{d_d^4}\left(\frac{c_d^2\eta^4}{4}+((c_d^2-1)\sin\eta+\sin\eta-\eta)^2\right).
\end{aligned}
$$

Using $|\sin\eta-\eta|\le|\eta|^3/6$ we obtain

$$
\begin{aligned}
||f_r(x)||^2 &\le \frac{V_r^2}{d_d^4}\left(\frac{c_d^2\eta^4}{4}+((c_d^2-1)\eta+\eta^3/6)^2\right)\\
&\le \frac{V_r^2}{d_d^4}\left(\frac{c_d^2\eta^2}{4}+((c_d^2-1)+\eta^2/6)^2\right)\eta^2\\
&\le \frac{V_r^2}{d_d^2}\left(\frac{c_d^2\eta^2}{4}+((c_d^2-1)+c_d^2/6)^2\right)x_1^2\\
&\le \frac{V_r^2}{d_d^2}\underbrace{\left(\frac{c_d^4}{4}+((c_d^2-1)+c_d^2/6)^2\right)}_{\le 2c_d^4}x_1^2\\
&\le 2\frac{V_r^2}{d_d^2}c_d^4x_1^2.
\end{aligned}
$$

Therefore, Eq. 24 follows immediately.

Finally, we need to show that the following bound holds

$$
||f_o(x)|| \le \frac{V_{o,\max}c_d}{d_d^2}\sqrt{1+c_d^2}. \tag{25}
$$

To this end, we write

$$
\begin{aligned}
||f_o(x)|| &\le \sqrt{V_o^2x_2^2/d_d^2+V_o^2x_2^4}\\
&\le \frac{V_{o,\max}x_2}{d_d}\sqrt{1+d_d^2x_2^2},
\end{aligned}
$$

which, using the fact that $||x||\le\frac{c_d}{d_d}$, can be rewritten as (25). This completes the proof.

References

1. Introduction to TCAS II, version 7.1. Federal Aviation Administration (2011)
2. Automatic dependent surveillance-broadcast (ads-b). Federal Aviation Administration. Available at, https://www.faa.gov/nextgen/programs/adsb/
3. Spriesterbach, T.P., Bruns, K.A., Baron, L.I., Sohlke, J.E.: Unmanned aircraft system airspace integration in the national airspace using a ground-based sense and avoid system. J. Hopkins APL Tech. Dig. **32**(3), 572–583 (2013)
4. Lyu, Y., Pan, Q., Zhao, C., Yu, C., Hu, J.: A UAV sense and avoid system design method based on software simulation. In: 2016 International Conference on Unmanned Aircraft Systems (ICUAS), pp. 572–579. IEEE (2016)
5. Sivaraman, S., Trivedi, M.M.: Looking at vehicles on the road: a survey of vision-based vehicle detection, tracking, and behavior analysis. IEEE Trans. Intell. Transp. Syst. **14**(4), 1773–1795 (2013)
6. Adán, A., Quintana, B., Vázquez, A.S., Olivares, A., Parra, E., Prieto, S.: Towards the automatic scanning of indoors with robots. Sensors **15**(5), 11551–11574 (2015)
7. Reina, G., Johnson, D., Underwood, J.: Radar sensing for intelligent vehicles in urban environments. Sensors **15**(6), 14661–14678 (2015)
8. Kochenderfer, M.J., Griffith, J.D., Kuchar, J.K.: Hazard alerting using line-of-sight rate. In: AIAA guidance, navigation, and control conference and exhibit (2008)
9. Albaker, B.M., Rahim, N.A.: Unmanned aircraft collision detection and resolution: concept and survey. In: 2010 the 5th IEEE Conference on Industrial Electronics and Applications (ICIEA), pp. 248–253. IEEE (2010)
10. Rozantsev, A., Lepetit, V., Fua, P.: Flying objects detection from a single moving camera. arXiv preprint arXiv:1411.7715 (2014)
11. Leitmann, G., Skowronski, J.M.: Avoidance control. J. Optim. Theory Appl. **23**, 581–591 (1977)
12. Moravec, H.: Certainty grids for mobile robots. In: Proceedings of the NASA/JPL Space Telerobotics Workshop, vol. 1, pp. 307–312 (1987)
13. Borenstein, J., Koren, Y.: The vector field histogram-fast obstacle avoidance for mobile robots. IEEE Trans. Robot. Autom. **7**(3), 278–288 (1991)
14. Khatib, O., Yokoi, K., Brock, O., Chang, K.-S., Casal, A.: Robots in human environments: Basic autonomous capabilities. Int. J. Robot. Res. **18**(7), 684–696 (1999)
15. Chakravarthy, A., Ghose, D.: Obstacle avoidance in a dynamic environment: a collision cone approach. IEEE Trans. Syst. Man Cybern. **28**(5), 562–574 (1998)
16. Fasano, G., Accardo, D., Moccia, A., Carbone, C., Ciniglio, U., Corraro, F., Luongo, S.: Multi-sensor-based fully autonomous non-cooperative collision avoidance system for unmanned air vehicles. J. Aerosp. Comput. Inf. Commun. **5**(10), 338–360 (2008)
17. Stipanović, D.M., Melikyan, A., Hovakimyan, N.: Guaranteed strategies for nonlinear multi-player pursuit-evasion games. Int. Game Theory Rev. **12**, 1–17 (2010)
18. Shankaran, S., Stipanović, D.M., Tomlin, C.J.: Collision avoidance strategies for a three-player game. In: Advances in Dynamic Games, pp. 253–271. Springer (2011)
19. Isaacs, R.: Differential games: a mathematical theory with applications to warfare and pursuit, control and optimization. Courier Corporation (1999)
20. Rodriguez-Seda, E.J., Stipanovic, D.M., Spong, M.W.: Collision avoidance control with sensing uncertainties. In: American Control Conference (ACC), 2011, pp. 3363–3368. IEEE (2011)

21. Panagou, D., Stipanović, D.M., Voulgaris, P.G.: Vision–based dynamic coverage control for nonholonomic agents. In: Proceedings of the 53rd IEEE Conference on Decision and Control. IEEE, Los Angeles (2014)
22. Hexsel, B., Chakraborty, N., Sycara, K.: Distributed coverage control for mobile anisotropic sensor networks. Robotics Institute, Pittsburgh, PA, Tech. Rep. CMU-RI-TR-13-01 (2013)
23. Gusrialdi, A., Hatanaka, T., Fujita, M.: Coverage control for mobile networks with limited-range anisotropic sensors. In: 47th IEEE Conference on Decision and Control, 2008. CDC 2008, pp. 4263–4268. IEEE (2008)
24. Laventall, K., Cortés, J.: Coverage control by robotic networks with limited-range anisotropic sensory. In: American Control Conference, 2008, pp. 2666–2671. IEEE (2008)
25. George, J., Ghose, D.: A reactive inverse pn algorithm for collision avoidance among multiple unmanned aerial vehicles. In: American Control Conference, 2009. ACC'09, pp. 3890–3895. IEEE (2009)
26. Elfes, A.: Using occupancy grids for mobile robot perception and navigation. Computer **22**(6), 46–57 (1989)
27. Khatib, O.: Real-time obstacle avoidance for manipulators and mobile robot. Int. J. Robot. Res. **5**(1), 90–98 (1986)
28. Khatib, O., Yokoi, K., Chang, K.-S., Ruspini, D., Holmberg, R., Casal, A.: Coordination and decentralized cooperation of multiple mobile manipulators. J. Robot. Syst. **13**(11), 755–764 (1996)
29. Smith, A., Coulter, D., Jones, C.: UAS collision encounter modeling and avoidance algorithm development for simulating collision avoidance. In: AIAA Modeling and Simulation Technologies Conference and Exhibit. Honolulu. AIAA-2008-7043 (2008)
30. Lee, B.H., Jeon, J.D., Oh, J.H.: Velocity obstacle based local collision avoidance for a holonomic elliptic robot. Auton. Robot, 1–17 (2016). doi:10.1007/s10514-016-9580-2
31. Exarchos, I., Tsiotras, P., Pachter, M.: UAV collision avoidance based on the solution of the suicidal pedestrian differential game. In: AIAA Guidance, Navigation, and Control Conference. San Diego, CA (2016)
32. Tripathi, A.K., Padhi, R.: Reactive collision avoidance of UAVs with simple pin-hole camera based passive stereovision sensing. Unmanned Syst. 1–25 (2016)
33. Degen, S.C.: Reactive image-based collision avoidance system for unmanned aircraft systems. PhD thesis, Queensland University of Technology (2011)
34. Shakernia, O., Chen, W.-Z., Raska, V.M.: Passive ranging for UAV sense and avoid applications. AIAA's Infotech at Aerospace (2005)
35. Voos, H.: UAV "see and avoid"? with nonlinear filtering and non-cooperative avoidance. In: Proceedings of the 13th IASTED International Conference Robotics and Applications. Wurzburg, Germany (2007)
36. Sharma, R., Saunders, J.B., Beard, R.W.: Reactive path planning for micro air vehicles using bearing-only measurements. J. Intell. Robot. Syst. **65**(1–4), 409–416 (2012)
37. Kurohmaru, M.: Area expansion apparatus, area expansion method, and area expansion program. US Patent 6,934,336 (2005)
38. Cichella, V., Marinho, T., Stipanović, D.M., Hovakimyan, N., Kaminer, I., Trujillo, A.: Collision avoidance based on line-of-sight angle. In: 2015 54th IEEE Conference on Decision and Control (CDC), pp. 6779–6784. IEEE (2015)
39. Dobrokhodov, V., Kaminer, I., Jones, K., Ghabcheloo, R.: Vision-based tracking and motion estimation for moving targets using unmanned air vehicles. J. Guid. Control. Dyn. **31**(4), 907–917 (2008)
40. Cichella, V., Kaminer, I., Dobrokhodov, V., Hovakimyan, N.: Cooperative vision based tracking of multiple UAVs. In: AIAA Guidance, Navigation, and Control Conference and Exhibit (2013)
41. Xargay, E., Kaminer, I., Pascoal, A., Hovakimyan, N., Dobrokhodov, V., Cichella, V., Pedro Aguiar, A., Ghabcheloo, R.: Time-critical cooperative path following of multiple unmanned aerial vehicles over time-varying networks. J. Guid. Control. Dyn. **36**(2), 499–516 (2013)
42. Cichella, V., Kaminer, I., Dobrokhodov, V., Xargay, E., Choe, R., Hovakimyan, N., Aguiar, A.P., Pascoal, A.M.: Cooperative path following of multiple multirotors over time-varying networks. IEEE Trans. Autom. Sci. Eng. **12**(3), 945–957 (2015)
43. Ren, W., Beard, R.W.: Trajectory tracking for unmanned air vehicles with velocity and heading rate constraints. IEEE Trans. Control Syst. Technol. **12**(5), 706–716 (2004)
44. Cichella, V., Kaminer, I., Dobrokhodov, V., Hovakimyan, N.: Coordinated vision-based tracking for multiple UAVs. In: 2015 IEEE/RSJ International Conference on Intelligent Robots and Systems (IROS), pp. 656–661. IEEE (2015)

Venanzio Cichella (cichell2@illinois.edu) received his M.S. in Automation Engineering in 2011 from the University of Bologna. Before that he spent 9 month at TU Delft as an Erasmus student, and 1 year at the Naval Postgraduate School as a visiting scholar and research assistant. In 2011 he started working on control of autonomous vehicles at the Naval Postgraduate School. In 2012 he moved to the University of Illinois at Urbana-Champaign, where he is currently a Ph.D. candidate in the Department of Mechanical Engineering. In 2015, he received the Ross J. Martin Memorial Award from the College of Engineering at UIUC for outstanding research achievement by a graduate student. His research interests include cooperative control of autonomous aerial and ground robots, nonlinear systems, robust and adaptive control, human-centered robotic design, and human-robot interaction.

Thiago Marinho is a PhD student in Mechanical Engineering at the University of Illinois at Urbana-Champaign. He received his MS degree in Control and Automation Engineering from the Ecole Centrale de Lille, France. Current interests include control theory, state estimation and mobile robotics.

Dušan Stipanović received his B.S. degree in electrical engineering from the University of Belgrade, Belgrade, Serbia, in 1994, and the M.S.E.E. and Ph.D. degrees (under supervision of Professor Dragoslav Šiljak) in electrical engineering from Santa Clara University, Santa Clara, California, in 1996 and 2000, respectively. Dr. Stipanović had been an Adjunct Lecturer and Research Associate with the Department of Electrical Engineering at Santa Clara University (1998–2001), and a Research Associate in Professor Claire Tomlin's Hybrid Systems Laboratory of the Department of Aeronautics and Astronautics at Stanford University (2001–2004). In 2004 he joined the University of Illinois at Urbana-Champaign where he is now Associate Professor in the Department of Industrial and Enterprise Systems Engineering and Coordinated Science Laboratory. He is a visiting Professor in the School of Electrical Engineering, University of Belgrade, Serbia, and in the Robotics and Telematics Department at the University of Wuerzburg, Germany, and also held a visiting faculty position in the EECS Department at the University of California at Berkeley. His research interests include decentralized control and estimation, stability theory, optimal control, and dynamic games with applications in control of autonomous vehicles, circuits, and medical robotics. Dr. Stipanović served as an Associate Editor on the Editorial Boards of the IEEE Transactions on Circuits and Systems I and II. Currently he is an Associate Editor for Journal of Optimization Theory and Applications.

Naira Hovakimyan received her MS degree in Theoretical Mechanics and Applied Mathematics in 1988 from Yerevan State University in Armenia. She got her Ph.D. in Physics and Mathematics in 1992, in Moscow, from the Institute of Applied Mathematics of Russian Academy of Sciences, majoring in optimal control and differential games. Before joining the faculty of UIUC in 2008, she has spent time as a research scientist at Stuttgart University in Germany, at INRIA in France, at Georgia Institute of Technology, and she was on faculty of Aerospace and Ocean Engineering of Virginia Tech during 2003-2008. She is currently W. Grafton and Lillian B. Wilkins Professor of Mechanical Science and Engineering at UIUC. In 2015 she was named as inaugural director for Intelligent Robotics Lab of CSL at UIUC. She has co-two books and more than 300 refereed publications. She is the recipient of the SICE International scholarship for the best paper of a young investigator in the VII ISDG Symposium (Japan, 1996), the 2011 recipient of AIAA Mechanics and Control of Flight award and the 2015 recipient of SWE Achievement Award. In 2014 she was awarded the Humboldt prize for her lifetime achievements and was recognized as Hans Fischer senior fellow of Technical University of Munich. In 2015 she was recognized by UIUC Engineering Council award for Excellence in Advising. She is a Fellow and life member of AIAA, a Senior Member of IEEE, and a member of SIAM, AMS, SWE, ASME and ISDG. Her work in robotics for elderly care was featured in the New York Times, on Fox TV and CNBC. Her research interests are in control and optimization, autonomous systems, neural networks, game theory and applications of those in aerospace, mechanical, agricultural, electrical, petroleum and biomedical engineering.

Isaac Kaminer received his Ph.D. in Electrical Engineering from University of Michigan in 1992. Before that he spent four years working at Boeing Commercial first as a control engineer in 757/767/747-400 Flight Management Computer Group and then as an engineer in Flight Control Research Group. Since 1992 he has been with the Naval Postgraduate School first at the Aeronautics and Astronautics Department and currently at the Department of Mechanical and Aerospace Engineering where he is a Professor. He has a total of over 20 years of experience in development and flight testing of guidance, navigation and control algorithms for both manned and unmanned aircraft. His more recent efforts were focused on development of coordinated control strategies for multiple UAVs and vision based guidance laws for a single UAV. Professor Kaminer has coauthored more than a hundred refereed publications. Over the years his research has been supported by ONR, NASA, US Army, NAVAIR and USSOCOM.

Anna Trujillo works at NASA Langley Research Center in the Crew Systems and Aviation Operations Branch. She graduated with a Master's in Aerospace Engineering from the University of Michigan and a Bachelor's in Aeronautical and Astronautical Engineering from the Massachusetts Institute of Technology. For both degrees, Anna Trujillo focused on human factors with a sub-focus on controls. Her research at NASA Langley Research Center has involved informational and alerting displays on aircraft systems and aircraft predicted health. Ms. Trujillo was involved with the NASA Langley Research Center's Autonomy Incubator where she focused on natural language use for control of autonomous agents. She has also worked on modeling the operator as an adaptive controller in order to better model, understand, and predict the operator's interaction with the aircraft. Anna Trujillo is currently back with NASA's UAS in the NAS program involving integrating Unmanned Aerial Systems into the National Airspace System. She is also busy planning research involving the requirements to use autonomous UAVs as a tool to further NASA's upcoming project on Autonomous Systems.